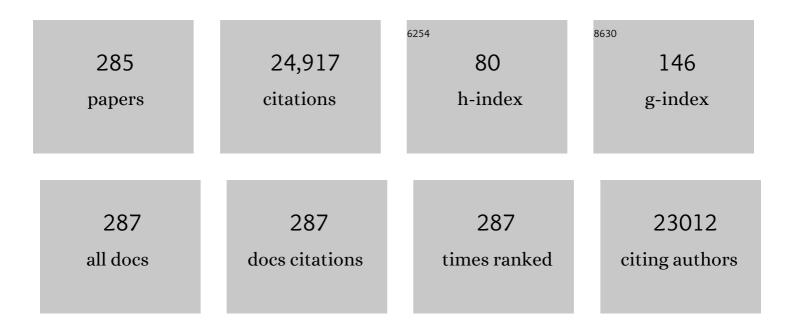
List of Publications by Year in descending order

Source: https://exaly.com/author-pdf/427913/publications.pdf Version: 2024-02-01



| # | Article | IF | CITATIONS |
|----|--|------|-----------|
| 1 | A Graphene Platform for Sensing Biomolecules. Angewandte Chemie - International Edition, 2009, 48, 4785-4787. | 13.8 | 1,801 |
| 2 | All-inorganic perovskite nanocrystal scintillators. Nature, 2018, 561, 88-93. | 27.8 | 1,274 |
| 3 | Simultaneous Fentonâ€like Ion Delivery and Clutathione Depletion by MnO ₂ â€Based Nanoagent to Enhance Chemodynamic Therapy. Angewandte Chemie - International Edition, 2018, 57, 4902-4906. | 13.8 | 1,068 |
| 4 | Synthesis of Copper Peroxide Nanodots for H ₂ O ₂ Self-Supplying Chemodynamic Therapy. Journal of the American Chemical Society, 2019, 141, 9937-9945. | 13.7 | 759 |
| 5 | Multifunctional Fe ₃ O ₄ @Polydopamine Core–Shell Nanocomposites for Intracellular mRNA Detection and Imaging-Guided Photothermal Therapy. ACS Nano, 2014, 8, 3876-3883. | 14.6 | 599 |
| 6 | Photoacoustic Imaging: Contrast Agents and Their Biomedical Applications. Advanced Materials, 2019, 31, e1805875. | 21.0 | 468 |
| 7 | Functional nucleic acid-based hydrogels for bioanalytical and biomedical applications. Chemical Society Reviews, 2016, 45, 1410-1431. | 38.1 | 416 |
| 8 | Self-assembly of DNA Nanohydrogels with Controllable Size and Stimuli-Responsive Property for Targeted Gene Regulation Therapy. Journal of the American Chemical Society, 2015, 137, 1412-1415. | 13.7 | 406 |
| 9 | Turn-On Fluorescence Sensor for Intracellular Imaging of Glutathione Using g-C ₃ N ₄ Nanosheet–MnO ₂ Sandwich Nanocomposite. Analytical Chemistry, 2014, 86, 3426-3434. | 6.5 | 378 |
| 10 | High-resolution X-ray luminescence extension imaging. Nature, 2021, 590, 410-415. | 27.8 | 378 |
| 11 | Metal Halide Perovskite Nanosheet for X-ray High-Resolution Scintillation Imaging Screens. ACS Nano, 2019, 13, 2520-2525. | 14.6 | 346 |
| 12 | Using graphene to protect DNA from cleavage during cellular delivery. Chemical Communications, 2010, 46, 3116. | 4.1 | 339 |
| 13 | Engineering Target-Responsive Hydrogels Based on Aptamerâ^'Target Interactions. Journal of the American Chemical Society, 2008, 130, 6320-6321. | 13.7 | 324 |
| 14 | Graphitic-phase C3N4 nanosheets as efficient photosensitizers and pH-responsive drug nanocarriers for cancer imaging and therapy. Journal of Materials Chemistry B, 2014, 2, 1031. | 5.8 | 298 |
| 15 | Functionalization of metal nanoclusters for biomedical applications. Analyst, The, 2016, 141, 3126-3140. | 3.5 | 279 |
| 16 | Ultrasoundâ€Activated Sensitizers and Applications. Angewandte Chemie - International Edition, 2020, 59, 14212-14233. | 13.8 | 271 |
| 17 | Co ₉ Se ₈ Nanoplates as a New Theranostic Platform for Photoacoustic/Magnetic Resonance Dualâ€Modalâ€Imagingâ€Guided Chemoâ€Photothermal Combination Therapy. Advanced Materials, 2015, 27, 3285-3291. | 21.0 | 265 |
| 18 | Protein Recognition via Surface Molecularly Imprinted Polymer Nanowires. Analytical Chemistry, 2006, 78, 317-320. | 6.5 | 251 |

| # | Article | IF | CITATIONS |
|----|--|------|-----------|
| 19 | An Ultrasound Activated Vesicle of Janus Auâ€MnO Nanoparticles for Promoted Tumor Penetration and Sonoâ€Chemodynamic Therapy of Orthotopic Liver Cancer. Angewandte Chemie - International Edition, 2020, 59, 1682-1688. | 13.8 | 249 |
| 20 | Mussel-inspired molecularly imprinted polymer coating superparamagnetic nanoparticles for protein recognition. Journal of Materials Chemistry, 2010, 20, 880-883. | 6.7 | 247 |
| 21 | Organic phosphors with bright triplet excitons for efficient X-ray-excited luminescence. Nature Photonics, 2021, 15, 187-192. | 31.4 | 237 |
| 22 | X-ray-activated nanosystems for theranostic applications. Chemical Society Reviews, 2019, 48, 3073-3101. | 38.1 | 231 |
| 23 | Amplified Aptamerâ€Based Assay through Catalytic Recycling of the Analyte. Angewandte Chemie - International Edition, 2010, 49, 8454-8457. | 13.8 | 212 |
| 24 | Sensing HIV related protein using epitope imprinted hydrophilic polymer coated quartz crystal microbalance. Biosensors and Bioelectronics, 2012, 31, 439-444. | 10.1 | 212 |
| 25 | Graphitic Carbon Nitride Materials: Sensing, Imaging and Therapy. Small, 2016, 12, 5376-5393. | 10.0 | 195 |
| 26 | Simultaneous Fentonâ€like Ion Delivery and Glutathione Depletion by MnO ₂ â€Based Nanoagent to Enhance Chemodynamic Therapy. Angewandte Chemie, 2018, 130, 4996-5000. | 2.0 | 195 |
| 27 | Facile Synthesis of Enhanced Fluorescent Gold–Silver Bimetallic Nanocluster and Its Application for Highly Sensitive Detection of Inorganic Pyrophosphatase Activity. Analytical Chemistry, 2016, 88, 8886-8892. | 6.5 | 190 |
| 28 | Recent Progress in NIR-II Contrast Agent for Biological Imaging. Frontiers in Bioengineering and Biotechnology, 2019, 7, 487. | 4.1 | 183 |
| 29 | Increasing the Sensitivity and Singleâ€Base Mismatch Selectivity of the Molecular Beacon Using Graphene Oxide as the "Nanoquencher― Chemistry - A European Journal, 2010, 16, 4889-4894. | 3.3 | 181 |
| 30 | Silver Nanolabels-Assisted Ion-Exchange Reaction with CdTe Quantum Dots Mediated Exciton Trapping for Signal-On Photoelectrochemical Immunoassay of Mycotoxins. Analytical Chemistry, 2016, 88, 7858-7866. | 6.5 | 177 |
| 31 | Endogenous Labile Iron Pool-Mediated Free Radical Generation for Cancer Chemodynamic Therapy. Journal of the American Chemical Society, 2020, 142, 15320-15330. | 13.7 | 170 |
| 32 | Black Phosphorus Quantum Dots with Renal Clearance Property for Efficient Photodynamic Therapy. Small, 2018, 14, 1702815. | 10.0 | 168 |
| 33 | Lowâ€Dose Xâ€ray Activation of W(VI)â€Doped Persistent Luminescence Nanoparticles for Deepâ€Tissue Photodynamic Therapy. Advanced Functional Materials, 2018, 28, 1707496. | 14.9 | 167 |
| 34 | General Colorimetric Detection of Proteins and Small Molecules Based on Cyclic Enzymatic Signal Amplification and Hairpin Aptamer Probe. Analytical Chemistry, 2012, 84, 5309-5315. | 6.5 | 165 |
| 35 | A New Class of NIRâ€II Gold Nanoclusterâ€Based Protein Biolabels for Inâ€Vivo Tumorâ€Targeted Imaging. Angewandte Chemie - International Edition, 2021, 60, 1306-1312. | 13.8 | 155 |
| 36 | Yolk–Shell Nanostructures: Design, Synthesis, and Biomedical Applications. Advanced Materials, 2018, 30, 1704639. | 21.0 | 153 |

| # | Article | IF | CITATIONS |
|----|---|------|-----------|
| 37 | A Ratiometric Fluorescent Bioprobe Based on Carbon Dots and Acridone Derivate for Signal Amplification Detection Exosomal microRNA. Analytical Chemistry, 2018, 90, 8969-8976. | 6.5 | 153 |
| 38 | A mussel-inspired supramolecular hydrogel with robust tissue anchor for rapid hemostasis of arterial and visceral bleedings. Bioactive Materials, 2021, 6, 2829-2840. | 15.6 | 152 |
| 39 | Room-temperature synthesis of core–shell structured magnetic covalent organic frameworks for efficient enrichment of peptides and simultaneous exclusion of proteins. Chemical Communications, 2017, 53, 3649-3652. | 4.1 | 144 |
| 40 | Janus Nanoparticles: From Fabrication to (Bio)Applications. ACS Nano, 2021, 15, 6147-6191. | 14.6 | 140 |
| 41 | Topological insulator bismuth selenide as a theranostic platform for simultaneous cancer imaging and therapy. Scientific Reports, 2013, 3, 1998. | 3.3 | 137 |
| 42 | Self-Assembled Responsive Bilayered Vesicles with Adjustable Oxidative Stress for Enhanced Cancer Imaging and Therapy. Journal of the American Chemical Society, 2019, 141, 8158-8170. | 13.7 | 132 |
| 43 | Bioinspired Mineral–Organic Bone Adhesives for Stable Fracture Fixation and Accelerated Bone Regeneration. Advanced Functional Materials, 2020, 30, 1908381. | 14.9 | 130 |
| 44 | Hydrogen Gas from Inflammation Treatment to Cancer Therapy. ACS Nano, 2019, 13, 8505-8511. | 14.6 | 124 |
| 45 | Facile synthesis of enzyme–inorganic hybrid nanoflowers and their application as an immobilized trypsin reactor for highly efficient protein digestion. RSC Advances, 2014, 4, 13888-13891. | 3.6 | 123 |
| 46 | Facile synthesis of polydopamine-coated molecularly imprinted silica nanoparticles for protein recognition and separation. Biosensors and Bioelectronics, 2013, 47, 120-126. | 10.1 | 122 |
| 47 | Enzyme-Free and Label-Free Ultrasensitive Electrochemical Detection of Human Immunodeficiency Virus DNA in Biological Samples Based on Long-Range Self-Assembled DNA Nanostructures. Analytical Chemistry, 2012, 84, 8277-8283. | 6.5 | 120 |
| 48 | Highly Selective and Sensitive Electrochemiluminescence Biosensor for p53 DNA Sequence Based on Nicking Endonuclease Assisted Target Recycling and Hyperbranched Rolling Circle Amplification. Analytical Chemistry, 2016, 88, 5097-5103. | 6.5 | 118 |
| 49 | Dye-enhanced graphene oxide for photothermal therapy and photoacoustic imaging. Journal of Materials Chemistry B, 2013, 1, 5762. | 5.8 | 115 |
| 50 | A universal multicolor immunosensor for semiquantitative visual detection of biomarkers with the naked eyes. Biosensors and Bioelectronics, 2017, 87, 122-128. | 10.1 | 115 |
| 51 | Equipping Natural Killer Cells with Specific Targeting and Checkpoint Blocking Aptamers for Enhanced Adoptive Immunotherapy in Solid Tumors. Angewandte Chemie - International Edition, 2020, 59, 12022-12028. | 13.8 | 114 |
| 52 | One-pot synthesis of an organic–inorganic hybrid affinity monolithic column for specific capture of glycoproteins. Chemical Communications, 2011, 47, 9675. | 4.1 | 108 |
| 53 | Semiautomated Support Photoelectrochemical Immunosensing Platform for Portable and High-Throughput Immunoassay Based on Au Nanocrystal Decorated Specific Crystal Facets BiVO ₄ Photoanode. Analytical Chemistry, 2016, 88, 12539-12546. | 6.5 | 107 |
| 54 | Yolk–Shell Nanostructure: An Ideal Architecture to Achieve Harmonious Integration of Magnetic–Plasmonic Hybrid Theranostic Platform. Advanced Materials, 2017, 29, 1606681. | 21.0 | 106 |

| # | Article | IF | CITATIONS |
|----|---|--------------------|-----------|
| 55 | Nongenetic Approach for Imaging Protein Dimerization by Aptamer Recognition and Proximity-Induced DNA Assembly. Journal of the American Chemical Society, 2018, 140, 4186-4190. | 13.7 | 106 |
| 56 | Amplified Visualization of Protein-Specific Glycosylation in Zebrafish via Proximity-Induced Hybridization Chain Reaction. Journal of the American Chemical Society, 2018, 140, 16589-16595. | 13.7 | 104 |
| 57 | A silk-based sealant with tough adhesion for instant hemostasis of bleeding tissues. Nanoscale Horizons, 2019, 4, 1333-1341. | 8.0 | 104 |
| 58 | Bispecific Aptamer Induced Artificial Protein-Pairing: A Strategy for Selective Inhibition of Receptor Function. Journal of the American Chemical Society, 2019, 141, 12673-12681. | 13.7 | 102 |
| 59 | Stimuliâ€Responsive Nanoparticles for Controlled Drug Delivery in Synergistic Cancer Immunotherapy. Advanced Science, 2022, 9, e2103444. | 11.2 | 102 |
| 60 | Protein-Metal Organic Framework Hybrid Composites with Intrinsic Peroxidase-like Activity as a Colorimetric Biosensing Platform. ACS Applied Materials & Interfaces, 2016, 8, 29052-29061. | 8.0 | 101 |
| 61 | Ultraselective Homogeneous Electrochemical Biosensor for DNA Species Related to Oral Cancer Based on Nicking Endonuclease Assisted Target Recycling Amplification. Analytical Chemistry, 2015, 87, 9204-9208. | 6.5 | 100 |
| 62 | Synthesis of uniformly sized molecularly imprinted polymer-coated silica nanoparticles for selective recognition and enrichment of lysozyme. Journal of Materials Chemistry, 2012, 22, 17914. | 6.7 | 99 |
| 63 | Ultrasound activation of liposomes for enhanced ultrasound imaging and synergistic gas and sonodynamic cancer therapy. Nanoscale Horizons, 2019, 4, 747-756. | 8.0 | 97 |
| 64 | An inorganic prodrug, tellurium nanowires with enhanced ROS generation and GSH depletion for selective cancer therapy. Chemical Science, 2019, 10, 7068-7075. | 7.4 | 97 |
| 65 | Selfâ€Assembled and Sizeâ€Controllable Oligonucleotide Nanospheres for Effective Antisense Gene Delivery through an Endocytosisâ€Independent Pathway. Angewandte Chemie - International Edition, 2019, 58, 5236-5240. | 13.8 | 97 |
| 66 | Molecularly imprinted polymer as SPE sorbent for selective extraction of melamine in dairy products. Talanta, 2009, 80, 821-825. | 5.5 | 96 |
| 67 | Cooperation of endogenous and exogenous reactive oxygen species induced by zinc peroxide nanoparticles to enhance oxidative stress-based cancer therapy. Theranostics, 2019, 9, 7200-7209. | 10.0 | 96 |
| 68 | A black phosphorus nanosheet-based siRNA delivery system for synergistic photothermal and gene therapy. Chemical Communications, 2018, 54, 3142-3145. | 4.1 | 93 |
| 69 | Two-dimensional tellurium nanosheets for photoacoustic imaging-guided photodynamic therapy. Chemical Communications, 2018, 54, 8579-8582. | 4.1 | 93 |
| 70 | Functionalizing Double-Network Hydrogels for Applications in Remote Actuation and in Low-Temperature Strain Sensing. ACS Applied Materials & Interfaces, 2020, 12, 30247-30258. | 8.0 | 93 |
| 71 | Mussel―and Barnacle Cement Proteinsâ€Inspired Dualâ€Bionic Bioadhesive with Repeatable Wetâ€Tissue Adhesion, Multimodal Selfâ€Healing, and Antibacterial Capability for Nonpressing Hemostasis and Promoted Wound Healing. Advanced Functional Materials, 2022, 32, . | 14.9 | 93 |
| 72 | Grapheneâ€Oxideâ€Modified Lanthanide Nanoprobes for Tumorâ€Targeted Visible/NIRâ€II Luminescence Imaging Angewandte Chemie - International Edition, 2019, 58, 18981-18986. | ^{5.} 13.8 | 92 |

| # | Article | IF | CITATIONS |
|----|---|------|-----------|
| 73 | A graphene oxide platform for energy transfer-based detection of protease activity. Biosensors and Bioelectronics, 2011, 26, 3894-3899. | 10.1 | 91 |
| 74 | Logicâ€Gateâ€Actuated DNAâ€Controlled Receptor Assembly for the Programmable Modulation of Cellular Signal Transduction. Angewandte Chemie - International Edition, 2019, 58, 18186-18190. | 13.8 | 90 |
| 75 | Copper Manganese Sulfide Nanoplates: A New Two-Dimensional Theranostic Nanoplatform for MRI/MSOT Dual-Modal Imaging-Guided Photothermal Therapy in the Second Near-Infrared Window. Theranostics, 2017, 7, 4763-4776. | 10.0 | 89 |
| 76 | Synthesis of boronic acid-functionalized molecularly imprinted silica nanoparticles for glycoprotein recognition and enrichment. Journal of Materials Chemistry B, 2014, 2, 637-643. | 5.8 | 88 |
| 77 | Nucleic Acids Analysis. Science China Chemistry, 2021, 64, 171-203. | 8.2 | 88 |
| 78 | Near-Infrared Light-Triggered Sulfur Dioxide Gas Therapy of Cancer. ACS Nano, 2019, 13, 2103-2113. | 14.6 | 86 |
| 79 | Facile Phase Transfer and Surface Biofunctionalization of Hydrophobic Nanoparticles Using Janus DNA Tetrahedron Nanostructures. Journal of the American Chemical Society, 2015, 137, 11210-11213. | 13.7 | 85 |
| 80 | Artificial chimeric exosomes for anti-phagocytosis and targeted cancer therapy. Chemical Science, 2019, 10, 1555-1561. | 7.4 | 85 |
| 81 | Manganese-iron layered double hydroxide: a theranostic nanoplatform with pH-responsive MRI contrast enhancement and drug release. Journal of Materials Chemistry B, 2017, 5, 3629-3633. | 5.8 | 83 |
| 82 | Dual Ratiometric SERS and Photoacoustic Core–Satellite Nanoprobe for Quantitatively Visualizing Hydrogen Peroxide in Inflammation and Cancer. Angewandte Chemie - International Edition, 2021, 60, 7323-7332. | 13.8 | 83 |
| 83 | A signal amplification electrochemical aptasensor for the detection of breast cancer cell via free-running DNA walker. Biosensors and Bioelectronics, 2016, 85, 184-189. | 10.1 | 80 |
| 84 | Biomimetic Design of Hollow Flowerâ€Like g 3N4@PDA Organic Framework Nanospheres for Realizing an Efficient Photoreactivity. Small, 2019, 15, e1900011. | 10.0 | 80 |
| 85 | Versatile surface engineering of porous nanomaterials with bioinspired polyphenol coatings for targeted and controlled drug delivery. Nanoscale, 2016, 8, 8600-8606. | 5.6 | 78 |
| 86 | Biologically Responsive Plasmonic Assemblies for Second Near-Infrared Window Photoacoustic Imaging-Guided Concurrent Chemo-Immunotherapy. ACS Nano, 2020, 14, 3991-4006. | 14.6 | 78 |
| 87 | Conductive Composite Fiber with Optimized Alignment Guides Neural Regeneration under Electrical Stimulation. Advanced Healthcare Materials, 2021, 10, e2000604. | 7.6 | 77 |
| 88 | A simple and ultrasensitive electrochemical DNA biosensor based on DNA concatamers. Chemical Communications, 2011, 47, 12116. | 4.1 | 76 |
| 89 | Gold Nanoparticle-Decorated g-C ₃ N ₄ Nanosheets for Controlled Generation of Reactive Oxygen Species upon 670 nm Laser Illumination. ACS Applied Materials & Interfaces, 2019, 11, 10589-10596. | 8.0 | 75 |
| 90 | NIR/ROSâ€Responsive Black Phosphorus QD Vesicles as Immunoadjuvant Carrier for Specific Cancer Photodynamic Immunotherapy. Advanced Functional Materials, 2020, 30, 1905758. | 14.9 | 75 |

| # | Article | IF | CITATIONS |
|-----|---|------|-----------|
| 91 | An ultrasensitive signal-on electrochemical aptasensor via target-induced conjunction of split aptamer fragments. Biosensors and Bioelectronics, 2010, 25, 996-1000. | 10.1 | 74 |
| 92 | Repeatable deep-tissue activation of persistent luminescent nanoparticles by soft X-ray for high sensitivity long-term in vivo bioimaging. Nanoscale, 2017, 9, 2718-2722. | 5.6 | 74 |
| 93 | DNA Octahedron-Based Fluorescence Nanoprobe for Dual Tumor-Related mRNAs Detection and Imaging. Analytical Chemistry, 2018, 90, 12059-12066. | 6.5 | 72 |
| 94 | Enhanced Cellular Ablation by Attenuating Hypoxia Status and Reprogramming Tumor-Associated Macrophages via NIR Light-Responsive Upconversion Nanocrystals. Bioconjugate Chemistry, 2018, 29, 928-938. | 3.6 | 71 |
| 95 | Bifunctional superparamagnetic surface molecularly imprinted polymer core-shell nanoparticles. Journal of Materials Chemistry, 2009, 19, 1077. | 6.7 | 70 |
| 96 | Polyphenolâ€Inspired Facile Construction of Smart Assemblies for ATP―and pHâ€Responsive Tumor MR/Optical Imaging and Photothermal Therapy. Small, 2017, 13, 1603997. | 10.0 | 70 |
| 97 | Single Wavelength Laser Excitation Ratiometric NIR-II Fluorescent Probe for Molecule Imaging in Vivo. Analytical Chemistry, 2020, 92, 6111-6120. | 6.5 | 70 |
| 98 | Silk fibroin-assisted exfoliation and functionalization of transition metal dichalcogenide nanosheets for antibacterial wound dressings. Nanoscale, 2017, 9, 17193-17198. | 5.6 | 69 |
| 99 | Smart Cu(II)-aptamer complexes based gold nanoplatform for tumor micro-environment triggered programmable intracellular prodrug release, photodynamic treatment and aggregation induced photothermal therapy of hepatocellular carcinoma. Theranostics, 2017, 7, 164-179. | 10.0 | 69 |
| 100 | Near-infrared light-mediated rare-earth nanocrystals: recent advances in improving photon conversion and alleviating the thermal effect. NPG Asia Materials, 2018, 10, 685-702. | 7.9 | 68 |
| 101 | Exonuclease-Catalyzed Target Recycling Amplification and Immobilization-free Electrochemical Aptasensor. Analytical Chemistry, 2015, 87, 11826-11831. | 6.5 | 66 |
| 102 | A novel colorimetric assay for rapid detection of cysteine and Hg2+ based on gold clusters. Talanta, 2016, 146, 71-74. | 5.5 | 65 |
| 103 | Recent Development in X-Ray Imaging Technology: Future and Challenges. Research, 2021, 2021, 9892152. | 5.7 | 65 |
| 104 | Singlet Oxygen Generation in Darkâ€Hypoxia by Catalytic Microenvironmentâ€Tailored Nanoreactors for NIRâ€II Fluorescenceâ€Monitored Chemodynamic Therapy. Angewandte Chemie - International Edition, 2021, 60, 15006-15012. | 13.8 | 64 |
| 105 | Water-Based Black Phosphorus Hybrid Nanosheets as a Moldable Platform for Wound Healing Applications. ACS Applied Materials & Interfaces, 2018, 10, 35495-35502. | 8.0 | 63 |
| 106 | Self-Quenched Metal–Organic Particles as Dual-Mode Therapeutic Agents for Photoacoustic Imaging-Guided Second Near-Infrared Window Photochemotherapy. ACS Applied Materials & Interfaces, 2018, 10, 25203-25212. | 8.0 | 63 |
| 107 | Ag ⁺ â€Coupled Black Phosphorus Vesicles with Emerging NIRâ€II Photoacoustic Imaging Performance for Cancer Immuneâ€Dynamic Therapy and Fast Wound Healing. Angewandte Chemie - International Edition, 2020, 59, 22202-22209. | 13.8 | 63 |
| 108 | Plasmonic-Fluorescent Janus Ag/Ag ₂ S Nanoparticles for <i>In Situ</i> H ₂ O ₂ -Activated NIR-II Fluorescence Imaging. Nano Letters, 2021, 21, 2625-2633. | 9.1 | 62 |

| # | Article | IF | CITATIONS |
|-----|---|------|-----------|
| 109 | Photogenerated Holes Mediated Nitric Oxide Production for Hypoxic Tumor Treatment. Angewandte Chemie - International Edition, 2021, 60, 7046-7050. | 13.8 | 61 |
| 110 | Chemotherapeutic Drug Based Metal–Organic Particles for Microvesicleâ€Mediated Deep Penetration and Programmable pH/NIR/Hypoxia Activated Cancer Photochemotherapy. Advanced Science, 2018, 5, 1700648. | 11.2 | 60 |
| 111 | GSHâ€Responsive Radiosensitizers with Deep Penetration Ability for Multimodal Imagingâ€Guided Synergistic Radioâ€Chemodynamic Cancer Therapy. Advanced Functional Materials, 2021, 31, 2101278. | 14.9 | 60 |
| 112 | Ultrasensitive detection of Cu2+ with the naked eye and application in immunoassays. NPG Asia Materials, 2012, 4, e10-e10. | 7.9 | 59 |
| 113 | Click synthesis of glucose-functionalized hydrophilic magnetic mesoporous nanoparticles for highly selective enrichment of glycopeptides and glycans. Journal of Chromatography A, 2014, 1358, 29-38. | 3.7 | 59 |
| 114 | Homogeneous electrochemical aptasensor for mucin 1 detection based on exonuclease I-assisted target recycling amplification strategy. Biosensors and Bioelectronics, 2018, 117, 474-479. | 10.1 | 59 |
| 115 | Dual-enhanced photothermal conversion properties of reduced graphene oxide-coated gold superparticles for light-triggered acoustic and thermal theranostics. Nanoscale, 2016, 8, 2116-2122. | 5.6 | 58 |
| 116 | Magnetic targeted near-infrared II PA/MR imaging guided photothermal therapy to trigger cancer immunotherapy. Theranostics, 2020, 10, 4997-5010. | 10.0 | 58 |
| 117 | Light-activated gold nanorod vesicles with NIR-II fluorescence and photoacoustic imaging performances for cancer theranostics. Theranostics, 2020, 10, 4809-4821. | 10.0 | 58 |
| 118 | Plant Polyphenolâ€Assisted Green Synthesis of Hollow CoPt Alloy Nanoparticles for Dualâ€Modality Imaging Guided Photothermal Therapy. Small, 2016, 12, 1506-1513. | 10.0 | 57 |
| 119 | Tumor Microenvironment Activable Selfâ€Assembled DNA Hybrids for pH and Redox Dualâ€Responsive Chemotherapy/PDT Treatment of Hepatocellular Carcinoma. Advanced Science, 2017, 4, 1600460. | 11.2 | 56 |
| 120 | Organic phosphorescent scintillation from copolymers by X-ray irradiation. Nature Communications, 2022, 13, . | 12.8 | 55 |
| 121 | Asymmetric Core–Shell Gold Nanoparticles and Controllable Assemblies for SERS Ratiometric Detection of MicroRNA. Angewandte Chemie - International Edition, 2021, 60, 12560-12568. | 13.8 | 54 |
| 122 | Graphene and Nanogoldâ€Functionalized Immunosensing Interface with Enhanced Sensitivity for Oneâ€Step Electrochemical Immunoassay of Alphaâ€Fetoprotein in Human Serum. Electroanalysis, 2010, 22, 2720-2728. | 2.9 | 53 |
| 123 | HCR-stimulated formation of DNAzyme concatamers on gold nanoparticle for ultrasensitive impedimetric immunoassay. Biosensors and Bioelectronics, 2015, 68, 487-493. | 10.1 | 53 |
| 124 | Kiwifruit-like Persistent Luminescent Nanoparticles with High-Performance and in Situ Activable Near-Infrared Persistent Luminescence for Long-Term in Vivo Bioimaging. ACS Applied Materials & Interfaces, 2017, 9, 41181-41187. | 8.0 | 51 |
| 125 | Broadband Detection of Xâ€ray, Ultraviolet, and Nearâ€Infrared Photons using Solutionâ€Processed Perovskite–Lanthanide Nanotransducers. Advanced Materials, 2021, 33, e2101852. | 21.0 | 51 |
| 126 | Near-Infrared II Gold Nanocluster Assemblies with Improved Luminescence and Biofate for In Vivo Ratiometric Imaging of H ₂ S. Analytical Chemistry, 2022, 94, 2641-2647. | 6.5 | 51 |

| # | Article | IF | CITATIONS |
|-----|--|------|-----------|
| 127 | Targeted photothermal ablation of pathogenic bacterium, Staphylococcus aureus, with nanoscale reduced graphene oxide. Journal of Materials Chemistry B, 2013, 1, 2496. | 5.8 | 50 |
| 128 | Quantitative Photoacoustic Diagnosis and Precise Treatment of Inflammation In Vivo Using Activatable Theranostic Nanoprobe. Advanced Functional Materials, 2020, 30, 2001771. | 14.9 | 50 |
| 129 | Quantitative Assessment of Copper(II) in Wilson's Disease Based on Photoacoustic Imaging and Ratiometric Surface-Enhanced Raman Scattering. ACS Nano, 2021, 15, 3402-3414. | 14.6 | 50 |
| 130 | Recent Advances of Membrane-Cloaked Nanoplatforms for Biomedical Applications. Bioconjugate Chemistry, 2018, 29, 838-851. | 3.6 | 49 |
| 131 | Grafting of molecularly imprinted polymers from the surface of silica gel particles via reversible addition-fragmentation chain transfer polymerization: A selective sorbent for theophylline. Talanta, 2009, 79, 141-145. | 5.5 | 48 |
| 132 | One-pot preparation of glutathione–silica hybrid monolith for mixed-mode capillary liquid chromatography based on "thiol-ene―click chemistry. Journal of Chromatography A, 2014, 1355, 228-237. | 3.7 | 48 |
| 133 | High-efficiency X-ray luminescence in Eu ³⁺ -activated tungstate nanoprobes for optical imaging through energy transfer sensitization. Nanoscale, 2018, 10, 1607-1612. | 5.6 | 48 |
| 134 | In Vivo Tracking of Cell Viability for Adoptive Natural Killer Cellâ€Based Immunotherapy by Ratiometric NIRâ€II Fluorescence Imaging. Angewandte Chemie - International Edition, 2021, 60, 20888-20896. | 13.8 | 48 |
| 135 | Graphitic carbon nitride supported platinum nanocomposites for rapid and sensitive colorimetric detection of mercury ions. Analytica Chimica Acta, 2017, 980, 72-78. | 5.4 | 47 |
| 136 | Homogeneous and label-free electrochemiluminescence aptasensor based on the difference of electrostatic interaction and exonuclease-assisted target recycling amplification. Biosensors and Bioelectronics, 2018, 105, 182-187. | 10.1 | 47 |
| 137 | A Highly Effective π–π Stacking Strategy To Modify Black Phosphorus with Aromatic Molecules for Cancer Theranostics. ACS Applied Materials & Interfaces, 2019, 11, 9860-9871. | 8.0 | 47 |
| 138 | In Vivo Xâ€ray Triggered Catalysis of H ₂ Generation for Cancer Synergistic Gas Radiotherapy. Angewandte Chemie - International Edition, 2021, 60, 12868-12875. | 13.8 | 47 |
| 139 | A colorimetric mercury(II) assay based on the Hg(II)-stimulated peroxidase mimicking activity of a nanocomposite prepared from graphitic carbon nitride and gold nanoparticles. Mikrochimica Acta, 2019, 186, 7. | 5.0 | 45 |
| 140 | Light-Switchable Yolk–Mesoporous Shell UCNPs@MgSiO ₃ for Nitric Oxide-Evoked Multidrug Resistance Reversal in Cancer Therapy. ACS Applied Materials & Interfaces, 2020, 12, 30066-30076. | 8.0 | 45 |
| 141 | Stimuli-Responsive Plasmonic Assemblies and Their Biomedical Applications. Nano Today, 2021, 36, 101014. | 11.9 | 45 |
| 142 | Nongenetic engineering strategies for regulating receptor oligomerization in living cells. Chemical Society Reviews, 2020, 49, 1545-1568. | 38.1 | 44 |
| 143 | High photoluminescent carbon based dots with tunable emission color from orange to green. Nanoscale, 2017, 9, 1028-1032. | 5.6 | 43 |
| 144 | Gadolinium oxysulfide-coated gold nanorods with improved stability and dual-modal magnetic resonance/photoacoustic imaging contrast enhancement for cancer theranostics. Nanoscale, 2017, 9, 56-61. | 5.6 | 43 |

| # | Article | IF | CITATIONS |
|-----|--|------|-----------|
| 145 | Artificial Engineered Natural Killer Cells Combined with Antiheat Endurance as a Powerful Strategy for Enhancing Photothermalâ€Immunotherapy Efficiency of Solid Tumors. Small, 2019, 15, e1902636. | 10.0 | 43 |
| 146 | Dyeâ€Sensitized Downconversion Nanoprobes with Emission Beyond 1500 nm for Ratiometric Visualization of Cancer Redox State. Advanced Functional Materials, 2021, 31, 2009942. | 14.9 | 43 |
| 147 | Structural Transformative Antioxidants for Dualâ€Responsive Antiâ€Inflammatory Delivery and Photoacoustic Inflammation Imaging. Angewandte Chemie - International Edition, 2021, 60, 14458-14466. | 13.8 | 43 |
| 148 | Organic Semiconductor Single Crystals for Xâ€ray Imaging. Advanced Materials, 2021, 33, e2104749. | 21.0 | 43 |
| 149 | Engineering of tungsten carbide nanoparticles for imaging-guided single 1,064 nm laser-activated dual-type photodynamic and photothermal therapy of cancer. Nano Research, 2018, 11, 4859-4873. | 10.4 | 42 |
| 150 | An oxidative stress-responsive electrospun polyester membrane capable of releasing anti-bacterial and anti-inflammatory agents for postoperative anti-adhesion. Journal of Controlled Release, 2021, 335, 359-368. | 9.9 | 42 |
| 151 | Direct detection of circulating microRNAs in serum of cancer patients by coupling protein-facilitated specific enrichment and rolling circle amplification. Chemical Communications, 2014, 50, 3292-3295. | 4.1 | 41 |
| 152 | Manganese-phenolic network-coated black phosphorus nanosheets for theranostics combining magnetic resonance/photoacoustic dual-modal imaging and photothermal therapy. Chemical Communications, 2019, 55, 850-853. | 4.1 | 40 |
| 153 | Switch-conversional ratiometric fluorescence biosensor for miRNA detection. Biosensors and Bioelectronics, 2020, 155, 112104. | 10.1 | 40 |
| 154 | Dual activated NIR-II fluorescence and photoacoustic imaging-guided cancer chemo-radiotherapy using hybrid plasmonic-fluorescent assemblies. Nano Research, 2020, 13, 3268-3277. | 10.4 | 39 |
| 155 | An Ultrasound Activated Vesicle of Janus Auâ€MnO Nanoparticles for Promoted Tumor Penetration and Sonoâ€Chemodynamic Therapy of Orthotopic Liver Cancer. Angewandte Chemie, 2020, 132, 1699-1705. | 2.0 | 38 |
| 156 | Cytosolic Delivery of Thiolated Mn GAMP Nanovaccine to Enhance the Antitumor Immune Responses. Small, 2021, 17, e2006970. | 10.0 | 38 |
| 157 | Magnetothermally Triggered Free-Radical Generation for Deep-Seated Tumor Treatment. Nano Letters, 2021, 21, 2926-2931. | 9.1 | 38 |
| 158 | Siteâ€Specific Biomimicry of Antioxidative Melanin Formation and Its Application for Acute Liver Injury Therapy and Imaging. Advanced Materials, 2021, 33, e2102391. | 21.0 | 38 |
| 159 | Nucleic acid-based molecular computation heads towards cellular applications. Chemical Society Reviews, 2021, 50, 12551-12575. | 38.1 | 38 |
| 160 | Simple colorimetric bacterial detection and high-throughput drug screening based on a graphene–enzyme complex. Nanoscale, 2013, 5, 619-623. | 5.6 | 36 |
| 161 | From Endocytosis to Nonendocytosis: The Emerging Era of Gene Delivery. ACS Applied Bio Materials, 2020, 3, 2686-2701. | 4.6 | 36 |
| 162 | Imaging of Receptor Dimers in Zebrafish and Living Cells via Aptamer Recognition and Proximity-Induced Hybridization Chain Reaction. Analytical Chemistry, 2018, 90, 14433-14438. | 6.5 | 35 |

| # | Article | IF | CITATIONS |
|-----|---|------|-----------|
| 163 | Enhancing Antitumor Efficacy by Simultaneous ATPâ€Responsive Chemodrug Release and Cancer Cell Sensitization Based on a Smart Nanoagent. Advanced Science, 2018, 5, 1801201. | 11.2 | 35 |
| 164 | A fast synthetic strategy for high-quality atomically thin antimonene with ultrahigh sonication power. Nano Research, 2018, 11, 5968-5977. | 10.4 | 35 |
| 165 | Self-Assembled mRNA-Responsive DNA Nanosphere for Bioimaging and Cancer Therapy in Drug-Resistant Cells. Analytical Chemistry, 2020, 92, 11779-11785. | 6.5 | 35 |
| 166 | DNA-mediated reversible capture and release of circulating tumor cells with a multivalent dual-specific aptamer coating network. Chemical Communications, 2019, 55, 5387-5390. | 4.1 | 34 |
| 167 | Cytosolic Delivery of Thiolated Neoantigen Nanoâ€Vaccine Combined with Immune Checkpoint Blockade to Boost Anti ancer T Cell Immunity. Advanced Science, 2021, 8, 2003504. | 11.2 | 34 |
| 168 | Ultrasound-propelled Janus Au NR-mSiO2 nanomotor for NIR-II photoacoustic imaging guided sonodynamic-gas therapy of large tumors. Science China Chemistry, 2021, 64, 2218-2229. | 8.2 | 34 |
| 169 | One-pot synthesis of phenylboronic acid-functionalized core-shell magnetic nanoparticles for selective enrichment of glycoproteins. RSC Advances, 2012, 2, 5062. | 3.6 | 33 |
| 170 | Sensitive fluorescence immunoassay of alpha-fetoprotein through copper ions modulated growth of quantum dots in-situ. Sensors and Actuators B: Chemical, 2017, 247, 408-413. | 7.8 | 33 |
| 171 | Bioinspired "Active―Stealth Magneto-Nanomicelles for Theranostics Combining Efficient MRI and Enhanced Drug Delivery. ACS Applied Materials & Interfaces, 2017, 9, 30502-30509. | 8.0 | 33 |
| 172 | Sensitive detection of telomerase activity in cancer cells using portable pH meter as readout. Biosensors and Bioelectronics, 2018, 121, 153-158. | 10.1 | 33 |
| 173 | Functional Self-Assembled DNA Nanohydrogels for Specific Telomerase Activity Imaging and Telomerase-Activated Antitumor Gene Therapy. Analytical Chemistry, 2020, 92, 15179-15186. | 6.5 | 33 |
| 174 | <i>In Situ</i> Activatable Ratiometric NIR-II Fluorescence Nanoprobe for Quantitative Detection of H ₂ S in Colon Cancer. Analytical Chemistry, 2021, 93, 9356-9363. | 6.5 | 33 |
| 175 | A novel sensitive detection platform for antitumor herbal drug aloe-emodin based on the graphene modified electrode. Talanta, 2010, 83, 553-558. | 5.5 | 32 |
| 176 | Label-free and ultrasensitive electrochemiluminescence detection of microRNA based on long-range self-assembled DNA nanostructures. Mikrochimica Acta, 2014, 181, 731-736. | 5.0 | 32 |
| 177 | Reducing PD-L1 expression with a self-assembled nanodrug: an alternative to PD-L1 antibody for enhanced chemo-immunotherapy. Theranostics, 2021, 11, 1970-1981. | 10.0 | 32 |
| 178 | Immobilization free electrochemical biosensor for folate receptor in cancer cells based on terminal protection. Biosensors and Bioelectronics, 2016, 86, 496-501. | 10.1 | 31 |
| 179 | Active Selfâ€Assembly of Trainâ€Shaped DNA Nanostructures via Catalytic Hairpin Assembly Reactions. Small, 2019, 15, e1901795. | 10.0 | 31 |
| 180 | Activatable nanoscale metal-organic framework for ratiometric photoacoustic imaging of hydrogen sulfide and orthotopic colorectal cancer in vivo. Science China Chemistry, 2020, 63, 1315-1322. | 8.2 | 31 |

| # | Article | IF | CITATIONS |
|-----|--|------|-----------|
| 181 | Wireless Optogenetic Modulation of Cortical Neurons Enabled by Radioluminescent Nanoparticles. ACS Nano, 2021, 15, 5201-5208. | 14.6 | 31 |
| 182 | A bioinspired mineral-organic composite hydrogel as a self-healable and mechanically robust bone graft for promoting bone regeneration. Chemical Engineering Journal, 2021, 413, 127512. | 12.7 | 30 |
| 183 | Quantum Dot-Based Sensitization System for Boosted Photon Absorption and Enhanced Second Near-Infrared Luminescence of Lanthanide-Doped Nanoparticle. Analytical Chemistry, 2020, 92, 6094-6102. | 6.5 | 29 |
| 184 | X-ray sensitive high-Z metal nanocrystals for cancer imaging and therapy. Nano Research, 2021, 14, 3744-3755. | 10.4 | 29 |
| 185 | An Activatable Hybrid Organic–Inorganic Nanocomposite as Early Evaluation System of Therapy Effect. Angewandte Chemie - International Edition, 2022, 61, . | 13.8 | 29 |
| 186 | A Graphene Platform for Sensitive Electrochemical Immunoassay of Carcinoembryoninc Antigen Based on Goldâ€Nanoflower Biolabels. Electroanalysis, 2011, 23, 832-841. | 2.9 | 28 |
| 187 | Multiplex detection of nucleases by a graphene-based platform. Journal of Materials Chemistry, 2011, 21, 10915. | 6.7 | 27 |
| 188 | Lightâ€Induced Activation of câ€Met Signalling by Photocontrolled DNA Assembly. Chemistry - A European Journal, 2018, 24, 15988-15992. | 3.3 | 27 |
| 189 | X-ray Nanocrystal Scintillator-Based Aptasensor for Autofluorescence-Free Detection. Analytical Chemistry, 2019, 91, 10149-10155. | 6.5 | 27 |
| 190 | Black Phosphorus Nanosheets for Killing Bacteria through Nanoknife Effect. Particle and Particle Systems Characterization, 2020, 37, 2000169. | 2.3 | 27 |
| 191 | Study on the electrochemical catalytic properties of the topological insulator Bi2Se3. Biosensors and Bioelectronics, 2013, 46, 171-174. | 10.1 | 25 |
| 192 | Switchable Bifunctional Stimuliâ€Triggered Polyâ€ <i>N</i> â€Isopropylacrylamide/DNA Hydrogels. Angewandte Chemie, 2014, 126, 10298-10302. | 2.0 | 24 |
| 193 | Unique Fluorescent Imaging Probe for Bacterial Surface Localization and Resistant Enzyme Imaging. ACS Chemical Biology, 2018, 13, 1890-1896. | 3.4 | 24 |
| 194 | Plasmonic gold nanoagents for cancer imaging and therapy. View, 2021, 2, 20200149. | 5.3 | 24 |
| 195 | A NO-Responsive Ratiometric Fluorescent Nanoprobe for Monitoring Drug-Induced Liver Injury in the Second Near-Infrared Window. Analytical Chemistry, 2021, 93, 15279-15287. | 6.5 | 24 |
| 196 | Aptamer-based self-assembled supramolecular vesicles for pH-responsive targeted drug delivery. Science China Chemistry, 2017, 60, 628-634. | 8.2 | 23 |
| 197 | A Simple Assay for Ultrasensitive Colorimetric Detection of Ag+ at Picomolar Levels Using Platinum Nanoparticles. Sensors, 2017, 17, 2521. | 3.8 | 23 |
| 198 | Selfâ€Assembled and Sizeâ€Controllable Oligonucleotide Nanospheres for Effective Antisense Gene Delivery through an Endocytosisâ€Independent Pathway. Angewandte Chemie, 2019, 131, 5290-5294. | 2.0 | 23 |

| # | Article | IF | CITATIONS |
|-----|---|------|-----------|
| 199 | Magnetic Nanomaterials for Magnetic Bioanalysis. , 2019, , 89-109. | | 23 |
| 200 | Autofluorescence-Free Immunoassay Using X-ray Scintillating Nanotags. Analytical Chemistry, 2018, 90, 6992-6997. | 6.5 | 22 |
| 201 | Light-Controlled, Toehold-Mediated Logic Circuit for Assembly of DNA Tiles. ACS Applied Materials & Interfaces, 2020, 12, 6336-6342. | 8.0 | 22 |
| 202 | An Activatable Xâ€Ray Scintillating Luminescent Nanoprobe for Early Diagnosis and Progression Monitoring of Thrombosis in Live Rat. Advanced Functional Materials, 2021, 31, 2006353. | 14.9 | 22 |
| 203 | Engineered Nanoscale Vanadium Metallodrugs for Robust Tumorâ€6pecific Imaging and Therapy. Advanced Functional Materials, 2021, 31, 2010337. | 14.9 | 22 |
| 204 | Highly Controlled Janus Organicâ€inorganic Nanocomposite as a Versatile Photoacoustic Platform. Angewandte Chemie - International Edition, 2021, 60, 17647-17653. | 13.8 | 22 |
| 205 | NIRâ€II Photoacoustic Reporter for Biopsyâ€Free and Realâ€Time Assessment of Wilson's Disease. Small, 2021, 17, e2008061. | 10.0 | 22 |
| 206 | Biodiversity and oil degradation capacity of oil-degrading bacteria isolated from deep-sea hydrothermal sediments of the South Mid-Atlantic Ridge. Marine Pollution Bulletin, 2021, 171, 112770. | 5.0 | 22 |
| 207 | Efficient detection of secondary structure folded nucleic acids related to Alzheimer's disease based on junction probes. Biosensors and Bioelectronics, 2012, 36, 142-146. | 10.1 | 21 |
| 208 | A facile approach for preparation of molecularly imprinted polymers layer on the surface of carbon nanotubes. Talanta, 2013, 105, 403-408. | 5.5 | 21 |
| 209 | Logicâ€Gateâ€Actuated DNAâ€Controlled Receptor Assembly for the Programmable Modulation of Cellular Signal Transduction. Angewandte Chemie, 2019, 131, 18354-18358. | 2.0 | 21 |
| 210 | One-pot synthesis of gold nanostars using plant polyphenols for cancer photoacoustic imaging and photothermal therapy. Journal of Nanoparticle Research, 2016, 18, 1. | 1.9 | 20 |
| 211 | Bifunctional magnetic nanoparticles for efficient cholesterol detection and elimination via host-guest chemistry in real samples. Biosensors and Bioelectronics, 2018, 120, 137-143. | 10.1 | 20 |
| 212 | Generating lung-metastatic osteosarcoma targeting aptamers for in vivo and clinical tissue imaging. Talanta, 2018, 188, 66-73. | 5.5 | 20 |
| 213 | Nanoformulation of metal complexes: Intelligent stimuli-responsive platforms for precision therapeutics. Nano Research, 2018, 11, 5474-5498. | 10.4 | 20 |
| 214 | An electrochemical sensor based on enzyme-free recycling amplification for sensitive and specific detection of miRNAs from cancer cells. Analyst, The, 2020, 145, 3353-3358. | 3.5 | 20 |
| 215 | FeOOH-loaded mesoporous silica nanoparticles as a theranostic platform with pH-responsive MRI contrast enhancement and drug release. Science China Chemistry, 2018, 61, 806-811. | 8.2 | 19 |
| 216 | Aluminium glycinate functionalized silica nanoparticles for highly specific separation of phosphoproteins. Journal of Materials Chemistry B, 2015, 3, 6528-6535. | 5.8 | 18 |

| # | Article | IF | CITATIONS |
|-----|---|------|-----------|
| 217 | Monodisperse phase transfer and surface bioengineering of metal nanoparticles via a silk fibroin protein corona. Nanoscale, 2017, 9, 2695-2700. | 5.6 | 18 |
| 218 | Semipermeable Functional DNA-Encapsulated Nanocapsules as Protective Bioreactors for Biosensing in Living Cells. Analytical Chemistry, 2017, 89, 5389-5394. | 6.5 | 18 |
| 219 | Reconstruction and evaluation of oil-degrading consortia isolated from sediments of hydrothermal vents in the South Mid-Atlantic Ridge. Scientific Reports, 2021, 11, 1456. | 3.3 | 18 |
| 220 | Target-induced biomolecular release for sensitive aptamer-based electrochemical detection of small molecules from magnetic graphene. RSC Advances, 2011, 1, 40. | 3.6 | 17 |
| 221 | Nearâ€Infrared Light Activated Thermosensitive Ion Channel to Remotely Control Transgene System for Thrombolysis Therapy. Small, 2019, 15, e1901176. | 10.0 | 17 |
| 222 | Equipping Natural Killer Cells with Specific Targeting and Checkpoint Blocking Aptamers for Enhanced Adoptive Immunotherapy in Solid Tumors. Angewandte Chemie, 2020, 132, 12120-12126. | 2.0 | 17 |
| 223 | Disulfide-Containing Molecular Sticker Assists Cellular Delivery of DNA Nanoassemblies by Bypassing Endocytosis. CCS Chemistry, 2021, 3, 1178-1186. | 7.8 | 17 |
| 224 | NIR-II Fluorescent Biodegradable Nanoprobes for Precise Acute Kidney/Liver Injury Imaging and Therapy. Analytical Chemistry, 2021, 93, 13893-13903. | 6.5 | 17 |
| 225 | Activated molecular probes for enzyme recognition and detection. Theranostics, 2022, 12, 1459-1485. | 10.0 | 17 |
| 226 | Polydopamine-mediated immobilization of phenylboronic acid on magnetic microspheres for selective enrichment of glycoproteins and glycopeptides. Science China Chemistry, 2015, 58, 1056-1064. | 8.2 | 16 |
| 227 | Circular DNA: a stable probe for highly efficient mRNA imaging and gene therapy in living cells. Chemical Communications, 2018, 54, 896-899. | 4.1 | 16 |
| 228 | Building Block Symmetry Relegation Induces Mesopore and Abundant Open-Metal Sites in Metal–Organic Frameworks for Cancer Therapy. CCS Chemistry, 2022, 4, 996-1006. | 7.8 | 16 |
| 229 | Improving the sensitivity of <i>T</i> ₁ contrast-enhanced MRI and sensitive diagnosing tumors with ultralow doses of MnO octahedrons. Theranostics, 2021, 11, 6966-6982. | 10.0 | 16 |
| 230 | Neodymium (3+)â€Coordinated Black Phosphorus Quantum Dots with Retrievable NIR/Xâ€Ray Optoelectronic Switching Effect for Antiâ€Glioblastoma. Small, 2022, 18, e2105160. | 10.0 | 15 |
| 231 | Activatable Nanoprobe with Aggregation-Induced Dual Fluorescence and Photoacoustic Signal Enhancement for Tumor Precision Imaging and Radiotherapy. Analytical Chemistry, 2022, 94, 5204-5211. | 6.5 | 15 |
| 232 | Acridone Derivate Simultaneously Featuring Multiple Functions and Its Applications. Analytical Chemistry, 2019, 91, 8406-8414. | 6.5 | 14 |
| 233 | Diversity of Cultivable Microbes From Soil of the Fildes Peninsula, Antarctica, and Their Potential Application. Frontiers in Microbiology, 2020, 11, 570836. | 3.5 | 14 |
| 234 | H ₂ O ₂ â€Responsive Nanogel for Enhancing Chemodynamic Therapy. ChemNanoMat, 2020, 6, 1054-1058. | 2.8 | 14 |

| # | Article | IF | CITATIONS |
|-----|---|-------------------|-----------|
| 235 | A New Class of NIRâ€II Gold Nanoclusterâ€Based Protein Biolabels for Inâ€Vivo Tumorâ€Targeted Imaging. Angewandte Chemie, 2021, 133, 1326-1332. | 2.0 | 14 |
| 236 | Multistage Cooperative Nanodrug Combined with PD‣1 for Enhancing Antitumor Chemoimmunotherapy. Advanced Healthcare Materials, 2021, 10, e2101199. | 7.6 | 14 |
| 237 | Systematic Interrogation of Cellular Signaling in Live Cells Using a Membraneâ€Anchored DNA Multitasking Processor. Angewandte Chemie - International Edition, 2022, 61, . | 13.8 | 14 |
| 238 | Spatial Regulation of Biomolecular Interactions with a Switchable Trident-Shaped DNA Nanoactuator. ACS Applied Materials & Interfaces, 2018, 10, 32579-32587. | 8.0 | 13 |
| 239 | Jungle on the Electrode: A Target-Induced Enzyme-Free and Label-Free Biosensor. Analytical Chemistry, 2019, 91, 13712-13719. | 6.5 | 13 |
| 240 | Emerging Plasmonic Assemblies Triggered by DNA for Biomedical Applications. Advanced Functional Materials, 2021, 31, 2005709. | 14.9 | 13 |
| 241 | Enhancing therapeutic effects and <i>in vivo</i> tracking of adipose tissue-derived mesenchymal stem cells for liver injury using bioorthogonal click chemistry. Nanoscale, 2021, 13, 1813-1822. | 5.6 | 13 |
| 242 | Singlet Oxygen Generation in Darkâ€Hypoxia by Catalytic Microenvironmentâ€Tailored Nanoreactors for NIRâ€II Fluorescenceâ€Monitored Chemodynamic Therapy. Angewandte Chemie, 2021, 133, 15133-15139. | 2.0 | 13 |
| 243 | DNA-Based Artificial Signaling System Mimicking the Dimerization of Receptors for Signal Transduction and Amplification. Analytical Chemistry, 2021, 93, 13807-13814. | 6.5 | 13 |
| 244 | Mesoporous radiosensitized nanoprobe for enhanced NIR-II photoacoustic imaging-guided accurate radio-chemotherapy. Nano Research, 2022, 15, 4154-4163. | 10.4 | 13 |
| 245 | siRNA-Based Carrier-Free System for Synergistic Chemo/Chemodynamic/RNAi Therapy of Drug-Resistant Tumors. ACS Applied Materials & Interfaces, 2022, 14, 361-372. | 8.0 | 13 |
| 246 | Grapheneâ€Oxideâ€Modified Lanthanide Nanoprobes for Tumorâ€Targeted Visible/NIRâ€II Luminescence Imaging Angewandte Chemie, 2019, 131, 19157-19162. | ^{5.} 2.0 | 12 |
| 247 | Novel electrochemical nanoswitch biosensor based on self-assembled pH-sensitive continuous circular DNA. Biosensors and Bioelectronics, 2019, 131, 274-279. | 10.1 | 12 |
| 248 | Rational design of a prodrug to inhibit self-inflammation for cancer treatment. Nanoscale, 2021, 13, 5817-5825. | 5.6 | 12 |
| 249 | Enzyme-free amplified detection of microRNA using target-catalyzed hairpin assembly and magnesium ion-dependent deoxyribozyme. Science China Chemistry, 2015, 58, 1906-1911. | 8.2 | 11 |
| 250 | Ultraschallaktivierte Sensibilisatoren. Angewandte Chemie, 2020, 132, 14316-14338. | 2.0 | 11 |
| 251 | DNA-Templated Glycan Labeling for Monitoring Receptor Spatial Distribution in Living Cells. Analytical Chemistry, 2021, 93, 12265-12272. | 6.5 | 11 |
| 252 | Aptamer-Induced-Dimerization Strategy Attenuates AβO Toxicity through Modulating the Trophic Activity of PrP ^C Signaling. Journal of the American Chemical Society, 2022, 144, 9264-9270. | 13.7 | 11 |

| # | Article | IF | CITATIONS |
|-----|---|-----------------------|--------------|
| 253 | Immunotherapy: Artificial Engineered Natural Killer Cells Combined with Antiheat Endurance as a Powerful Strategy for Enhancing Photothermalâ€Immunotherapy Efficiency of Solid Tumors (Small) Tj ETQq1 1 0. | .7 80-3 01.4 r | gBII0/Overlo |
| 254 | Asymmetric Core–Shell Gold Nanoparticles and Controllable Assemblies for SERS Ratiometric Detection of MicroRNA. Angewandte Chemie, 2021, 133, 12668-12676. | 2.0 | 10 |
| 255 | A Cyanineâ€Mediated Selfâ€Assembly System for the Construction of a Twoâ€inâ€One Nanodrug. Angewandte Chemie - International Edition, 2021, 60, 21226-21230. | 13.8 | 10 |
| 256 | In Vivo Tracking of Cell Viability for Adoptive Natural Killer Cellâ€Based Immunotherapy by Ratiometric NIRâ€II Fluorescence Imaging. Angewandte Chemie, 2021, 133, 21056-21064. | 2.0 | 10 |
| 257 | Host–guest assembly of adamantyl tethered squaraine in β-cyclodextrin for monitoring pH in living cells. RSC Advances, 2014, 4, 52690-52693. | 3.6 | 9 |
| 258 | Fullerene‣tructural Carbonâ€Based Dots from C ₆₀ Molecules and their Optical Properties. Particle and Particle Systems Characterization, 2016, 33, 916-923. | 2.3 | 9 |
| 259 | Multifunctional human serum albumin-modified reduced graphene oxide for targeted photothermal therapy of hepatocellular carcinoma. RSC Advances, 2016, 6, 11167-11175. | 3.6 | 9 |
| 260 | Photodynamic therapy: When van der Waals heterojunction meets tumor. Chemical Engineering Journal, 2021, 421, 129773. | 12.7 | 9 |
| 261 | Biodegradable Blackâ€Phosphorusâ€Nanosheetâ€Based Nanoagent for Enhanced Chemoâ€Photothermal Therapy. Particle and Particle Systems Characterization, 2020, 37, 2000243. | 2.3 | 8 |
| 262 | Multifunctional Carbon Monoxide Prodrug-Loaded Nanoplatforms for Effective Photoacoustic Imaging-Guided Photothermal/Gas Synergistic Therapy. ACS Applied Bio Materials, 2021, 4, 4557-4564. | 4.6 | 8 |
| 263 | Cellular transformers for targeted therapy. Advanced Drug Delivery Reviews, 2021, 179, 114032. | 13.7 | 8 |
| 264 | Flexible X-ray luminescence imaging enabled by cerium-sensitized nanoscintillators. Journal of Luminescence, 2022, 242, 118589. | 3.1 | 8 |
| 265 | Synergistic Silencing of Skp2 by siRNA Selfâ€Assembled Nanoparticles as a Therapeutic Strategy for Advanced Prostate Cancer. Small, 2022, 18, e2106046. | 10.0 | 8 |
| 266 | Dual inhibition of glycolysis and oxidative phosphorylation by aptamer-based artificial enzyme for synergistic cancer therapy. Nano Research, 2022, 15, 6278-6287. | 10.4 | 8 |
| 267 | Characterization of novel cyclic lipopeptides produced by Bacillus sp. SY27F. Process Biochemistry, 2019, 83, 206-213. | 3.7 | 7 |
| 268 | Spatiotemporal ontrolled Reporter for Cell‧urface Proteolytic Enzyme Activity Visualization. ChemBioChem, 2019, 20, 561-567. | 2.6 | 6 |
| 269 | Cytotoxic study in the treatment of tetracycline by using magnetic Fe3O4–PAMAM–antibody complexes. Environmental Chemistry Letters, 2019, 17, 543-549. | 16.2 | 6 |
| 270 | In Vivo Xâ€ray Triggered Catalysis of H 2 Generation for Cancer Synergistic Gas Radiotherapy. Angewandte Chemie, 2021, 133, 12978-12985. | 2.0 | 6 |

| # | Article | IF | CITATIONS |
|-----|--|------|-----------|
| 271 | Highly Controlled Janus Organicâ€Inorganic Nanocomposite as a Versatile Photoacoustic Platform. Angewandte Chemie, 2021, 133, 17788-17794. | 2.0 | 6 |
| 272 | Rational design of a hollow multilayer heterogeneous organic framework for photochemical applications. Materials Chemistry Frontiers, 2020, 4, 2646-2654. | 5.9 | 6 |
| 273 | An Activatable Hybrid Organic–Inorganic Nanocomposite as Early Evaluation System of Therapy Effect. Angewandte Chemie, 2022, 134, . | 2.0 | 6 |
| 274 | Bacilohydrin A, a New Cytotoxic Cyclic Lipopeptide of Surfactins Class Produced by <i>Bacillus</i> sp. SY27F from the Indian Ocean Hydrothermal Vent. Natural Product Communications, 2019, 14, 1934578X1901400. | 0.5 | 4 |
| 275 | Iron phosphide nanoparticles as a pH-responsive <i>T</i> ₁ contrast agent for magnetic resonance tumor imaging. RSC Advances, 2019, 9, 30581-30584. | 3.6 | 4 |
| 276 | Dual Ratiometric SERS and Photoacoustic Core–Satellite Nanoprobe for Quantitatively Visualizing Hydrogen Peroxide in Inflammation and Cancer. Angewandte Chemie, 2021, 133, 7399-7408. | 2.0 | 4 |
| 277 | A Perovskite-Based Paper Microfluidic Sensor for Haloalkane Assays. Frontiers in Chemistry, 2021, 9, 682006. | 3.6 | 4 |
| 278 | Structural Transformative Antioxidants for Dualâ€Responsive Antiâ€Inflammatory Delivery and Photoacoustic Inflammation Imaging. Angewandte Chemie, 2021, 133, 14579-14587. | 2.0 | 4 |
| 279 | Ag + â€Coupled Black Phosphorus Vesicles with Emerging NIRâ€II Photoacoustic Imaging Performance for Cancer Immuneâ€Dynamic Therapy and Fast Wound Healing. Angewandte Chemie, 2020, 132, 22386-22393. | 2.0 | 3 |
| 280 | Photogenerated Holes Mediated Nitric Oxide Production for Hypoxic Tumor Treatment. Angewandte Chemie, 2021, 133, 7122-7126. | 2.0 | 3 |
| 281 | Systematic Interrogation of Cellular Signaling in Live Cells Using a Membraneâ€Anchored DNA Multitasking Processor. Angewandte Chemie, 2022, 134, . | 2.0 | 3 |
| 282 | Selective and Nongenetic Peroxidase Tag of Membrane Protein: a Nucleic Acid Tool for Proximity Labeling. Analytical Chemistry, 2022, 94, 1101-1107. | 6.5 | 3 |
| 283 | A Cyanineâ€Mediated Selfâ€Assembly System for the Construction of a Twoâ€inâ€One Nanodrug. Angewandte Chemie, 2021, 133, 21396-21400. | 2.0 | 1 |
| 284 | Antithrombotic Therapies: Nearâ€Infrared Light Activated Thermosensitive Ion Channel to Remotely Control Transgene System for Thrombolysis Therapy (Small 27/2019). Small, 2019, 15, 1970146. | 10.0 | 0 |
| 285 | Upconversion Nanomaterials for Near-infrared Light-Mediated Theranostics. , 2019, , 321-340. | | 0 |